CLINICAL INVESTIGATIONS

STIM1 and *SLC24A4* Are Critical for Enamel Maturation

S.Wang[1,2], M. Choi[3,4]*, A.S. Richardson[1], B.M. Reid[1], F. Seymen[5], M. Yildirim[5], E. Tuna[5], K. Gençay[5], J.P. Simmer[1]*, and J.C. Hu[1]

APPENDIX

DOI: 10.1177/0022034514527971. [1]Department of Biologic and Materials Sciences, University of Michigan School of Dentistry, 1210 Eisenhower Place, Ann Arbor, MI, USA; [2]Oral Health Sciences Program, University of Michigan School of Dentistry, 1011 North University, Ann Arbor, MI, USA; [3]Department of Biomedical Sciences, College of Medicine, Seoul National University, 275-1 Yongon-dong, Chongno-gu, Seoul 110-768, Korea; [4]Department of Genetics, Howard Hughes Medical Institute, Yale University School of Medicine, 333 Cedar Street, New Haven, CT, USA; and [5]Department of Pedodontics, Istanbul University, Faculty of Dentistry, Istanbul, Turkey; *corresponding authors, jsimmer@umich.edu, murimchoi@snu.ac.kr

Appendix Figure 1.
STIM1 gene structure and disease-causing mutations. The 12 numbered boxes are exons. Introns are indicated by black lines (intron lengths are not drawn to scale). The numbers below each exon indicate the range of amino acids encoded by the exon. Above the gene diagrams, the locations of the 8 reported *STIM1* disease-causing mutations are indicated. The 4 most 5′ mutations caused autosomal-dominant Tubular-Aggregate Myopathy (TAM; MIM #160565) with no mention of tooth defects. These defects in the STIM1 EF hand constitutively activate STIM1. The 4 most 3′ mutations caused autosomal-recessive Immunodeficiency 10 (IMD10; MIM #612783), which inactivates STIM1. The gene structure diagram is based upon the *STIM1* genomic reference sequence (NG_016277.1) and the reference sequences of the 3 human cDNA transcript variants (tv) listed in GenBank (tv1: NM_001277961.1; tv2: NM_003156.3; tv3: NM_001277962.1). The cDNA descriptions of the mutations are based upon the tv1 reference sequence.

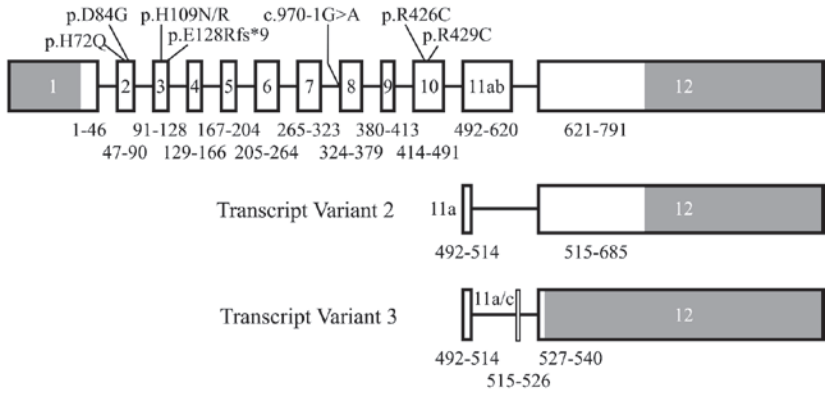

STIM1 mutations causing Tubular-Aggregate Myopathy (TAM; MIM #160565)

	Location	Gene	cDNA	Protein	Reference
1.	Exon 2	g.116924C>G	c.216C>G	p.His72Gln	(Bohm et al., 2013)
2.	Exon 2	g.116961A>G	c.251A>G	p.Asp84Gly	(Bohm et al., 2013)
3.	Exon 3	g.173225C>A	c.325C>A	p.His109Asn	(Bohm et al., 2013)
4.	Exon 3	g.173226A>G	c.326A>G	p.His109Arg	(Bohm et al., 2013)

STIM1 mutations causing Immunodeficiency 10 (IMD10; MIM #612783)

	Location	Gene	cDNA	Protein	Reference
5.	Exon 3	g.173281dup	c.381dup	p.Glu128Argfs*9	(Picard et al., 2009) (Feske et al., 2010)
6.	Intron 7	g.231481G>A	c.970-1G>A	p.-	(Byun et al., 2010)
7.	Exon 10	g.232598C>T	c.1276C>T	p.Arg426Cys	This Report
8.	Exon 10	g.232607C>T	c.1285C>T	p.Arg429Cys	(Fuchs et al., 2012)

Appendix Figure 2.
Dental features of patients with *STIM1* or *ORAI1* mutations. **(A)** Black-and-white oral photograph of the primary dentition of a proband with a homozygous *STIM1* (g.232607C>T c.1285C>T p.Arg429Cys) defect. [This image is reproduced from Fig. 1 of Fuchs *et al.* (2012) with permission from the publisher.] (**B)** Oral photograph of the primary mandibular teeth of a proband who was homozygous for a missense mutation in *ORAI1* (p.Arg91Trp), which is reproduced from Fig. 6 of Feske *et al.* (2010) with permission from the publisher. (**C)** This oral photograph is a frontal view from the same patient shown in (B). On the right are an oral photograph and a radiograph of posterior permanent teeth from the patient at a later age. [This Fig. was reproduced from Fig. 3 of McCarl *et al.* (2009) with permission from the publisher.] These are the only published oral photographs we could find of patients with *STIM1* or *ORAI1* defects.

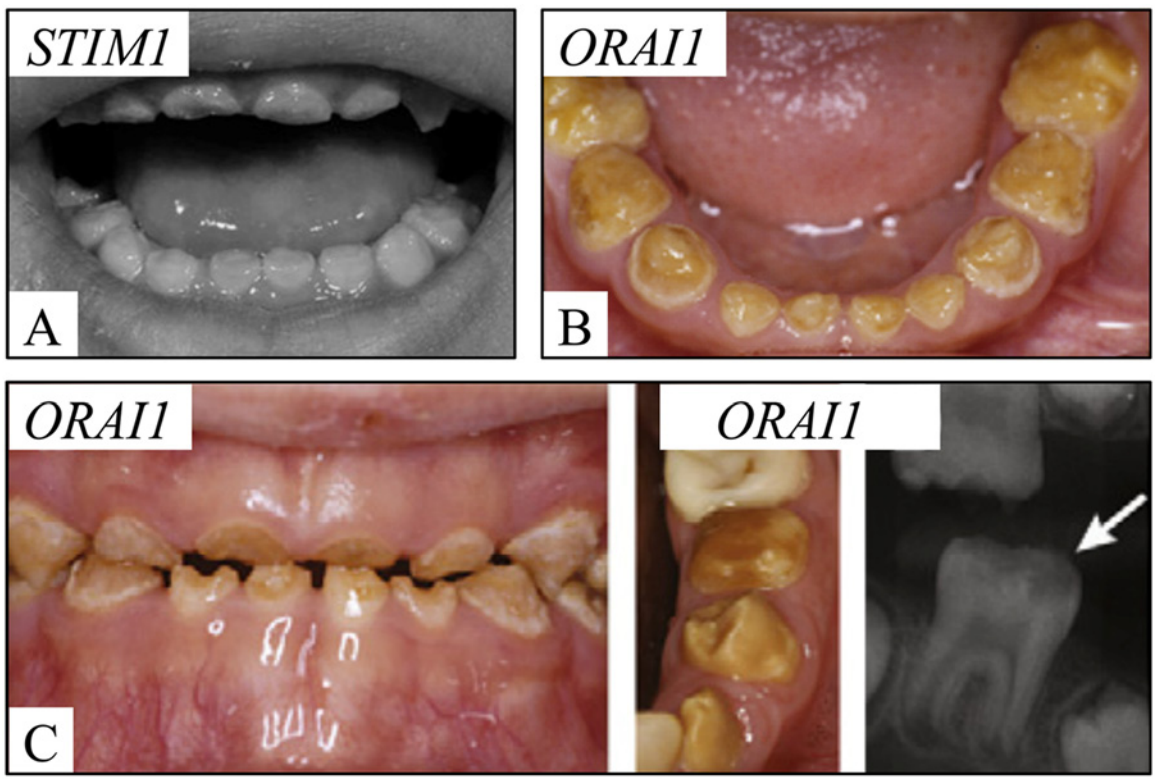

Appendix Figure 3.
The 8 novel rare protein-altering homozygous sequence variants identified in the proband by whole-exome sequencing and analysis. The *STIM1* variation (p.Arg426Cys) was determined to be disease-causing based upon the clinical phenotype of the proband. Enamel and nail malformations have been observed in other *STIM1* mutants, including a proband who had a similar *STIM1* missense mutation (p.Arg429Cys) only 3 amino acids away on the protein (Fuchs *et al.*, 2012). In addition, *in vitro* studies showed that mutation of Arg^{426} blocked a key functional interaction with ORAI1 (Muik *et al.*, 2011).

Gene	Full Name	HG19 Position	NT Δ	AA Δ
AGXT2	alanine–glyoxylate aminotransferase 2	35014109	G>A	A360V
COX4I2	cytochrome c oxidase subunit IV isoform 2	30231248	C>G	R97G
DLX6	distal-less homeobox 6	96639220	C>T	S248L
DNAH5	dynein, axonemal, heavy chain 5	13882900	C>T	A1067T
DNAJC21	DnaJ (Hsp40) homolog, subfamily C, member 21	34954668	T>C	I482T
PIEZO1	piezo-type mechanosensitive ion channel component 1	88804353	G>A	P337S
RELN	reelin	103162497	G>A	A2547V
STIM1	stromal interaction molecule 1	4104530	C>T	R426C

Appendix Figure 4.
Conservation of STIM1 Arg^{429} in vertebrates. **(A)** Alignment of STIM1 protein sequences from the human (*Homo sapiens*), mouse (*Mus musculus*), opossum (*Monodelphis domestica*), anole *(Anolis carolinensis),* chicken (*Gallus gallus*), frog (*Xenopus tropicalis*), and fish (*Danio rerio*). The arginine (Arg^{426}) changed to cysteine in our proband is in bold. The arginine (Arg^{429}) changed to cysteine in the proband of another study (Fuchs *et al.*, 2012) is underlined. **(B)** Ethidium-bromide-stained agarose gel showing RT-PCR amplification products of EOE from day 11 mouse first molars. The major amplification product was 503 base pairs (bp), analogous to human *STIM1* transcript variant 2 (tv2). A trace band at 596 contained a mixture of tv2 and a larger product containing a 93-bp segment from intron 10 that was bracketed by appropriate splice junctions, although this variant is not listed in GenBank. The PCR primers were F: CTCTGCGGTTTCCAGATTGT and R: ACTGAGGGGTTCAGCTCCAT.

A

Human	ILTAKQALSEVTAALRE**R**LHRWQQIEILCGFQIVNN
Mouse	ILTAKQALSEVTAALRE**R**LHRWQQIEILCGFQIVNN
Opossum	ILTAKQALSEVTAALRE**R**LHRWQQIEILCGFQIVNN
Anole	ILTAKQALSEVTAALRE**R**LHRWQQIEMLCGFQIVNN
Chicken	ILTAKQALSEVTAALRE**R**LHRWQQIELLCGFQIVNN
Frog	ILTAKQALSEVTAALRE**R**LHRWQQIETLCGFQIVNN
Fish	ILAAKQALGEVTAALRE**R**LHRWQQIELLTGFTLVHN

B

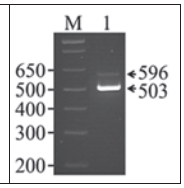

Appendix Figure 5.
Strict conservation of Ala[146] throughout phylogeny.

Gene	Species	Accession	Sequence
SLC24A1	H.sapiens	NP_004718.1	ISEDVAGATFMAAGGSAPELFTS
	P.troglodytes	XP_001174585.1	ISEDVAGATFMAAGGSAPELFTS
	M.mulatta	XP_001103481.2	ISEDVAGATFMAAGGSAPELFTS
	C.lupus	XP_003433931.1	ISDDVAGATFMAAGGSAPELFTS
	B.taurus	NP_777080.1	ISEDVAGATFMAAGGSAPELFTS
	M.musculus	NP_659062.1	ISEDVAGATFMAAGGSAPELFTS
	R.norvegicus	NP_064475.1	ISEDVAGATFMAAGGSAPELFTS
	C.elegans	NP_001040663.1	LSDDVAGATFMAAGGSAPEFFTS
	C.elegans	NP_505690.2	ISDDVAGATFMAAGGSAPEFFTS
SLC24A2	H.sapiens	NP_065077.1	ISDDVAGATFMAAGGSAPELFTS
	P.troglodytes	XP_528551.2	ISDDVAGATFMAAGGSAPELFTS
	M.mulatta	XP_001108751.1	ISDDVAGATFMAAGGSAPELFTS
	C.lupus	XP_852036.2	ISDDVAGATFMAAGGSAPELFTS
	B.taurus	NP_001137566.1	ISDDVAGATFMAAGGSAPELFTS
	M.musculus	NP_766014.1	ISDDVAGATFMAAGGSAPELFTS
	R.norvegicus	NP_113931.1	ISDDVAGATFMAAGGSAPELFTS
	G.gallus	NP_001001772.1	ISDDVAGATFMAAGGSAPELFTS
	D.melanogaster	NP_001188761.1	ITDDVAGATFMAAGGSAPELFTS
	A.gambiae	XP_555111.3	ITDDVAGATFMAAGGSAPELFTS
SLC24A3	H.sapiens	NP_065740.2	LSEDVAGATFMAAGSSAPELFTS
	M.mulatta	XP_001090485.2	LSEDVAGATFMAAGSSAPELFTS
	C.lupus	XP_849585.2	LSEDVAGATFMAAGSSAPELFTS
	B.taurus	XP_002692183.1	LSEDVAGATFMAAGSSAPELFTS
	M.musculus	NP_444425.1	LSEDVAGATFMAAGSSAPELFTS
	R.norvegicus	NP_445957.1	LSEDVAGATFMAAGSSAPELFTS
	G.gallus	XP_419316.3	LSEDVAGATFMAAGSSAPELFTS
	D.rerio	XP_685302.3	LSEDVAGATFMAAGSSAPELFTS
	D.melanogaster	NP_001015260.3	MSNDVAGATFMAAATSAPELFVN
	A.gambiae	XP_001688244.1	VKEDVAGATFMAAASSSPELFIN
SLC24A4	H.sapiens	NP_705932.2	LSEDVAGATFMAAGSSTPELFAS
	P.troglodytes	XP_522932.2	LSEDVAGATFMAAGSSTPELFAS
	M.mulatta	XP_001093162.2	LSEDVAGATFMAAGSSTPELFAS
	C.lupus	XP_849226.1	LSEDVAGATFMAAGSSTPELFAS
	B.taurus	NP_001180017.1	LSEDVAGATFMAAGSSTPELFAS
	M.musculus	NP_742164.1	LSEDVAGATFMAAGSSTPELFAS
	R.norvegicus	NP_001101521.1	LSEDVAGATFMAAGSSTPELFAS
	G.gallus	XP_001235438.1	LSEDVAGATFMAAGSSTPELFAS
	D.rerio	NP_001017770.1	LSEDVAGATFMAAGSSAPELFAS
	D.rerio	XP_002665845.1	LSEDVAGATFMAAGSSAPELFAS
	D.melanogaster	NP_649459.3	LSPDVAGATFMAAGSSAPELATV
	A.gambiae	XP_313818.3	LSPDVAGATFMAAGSSAPELATV
SLC24A5	H.sapiens	NP_995322.1	LSQDVAGTTFMAAGSSAPELVTA
	P.troglodytes	XP_510380.2	LSQDVAGATFMAAGSSAPELVTA
	M.mulatta	XP_001112601.1	LSQDVAGATFMAVGSSAPELVTA
	C.lupus	XP_851849.1	LSQDVAGATFMAAGSSAPELVTA
	B.taurus	NP_001121981.1	LSQDVAGATFMAAGSSAPELVTA
	M.musculus	NP_778199.2	LSQDVAGATFMAAGSSAPELVTA
	G.gallus	NP_001033586.2	LSQDVAGATFMAAGSSAPELVTA
	D.rerio	NP_001025451.1	LSQDVAGATFMAAGSSAPELVTA

(continued)

Appendix Figure 5.
(continued)

SLC8A1	H.sapiens	NP_066920.1	WNETVSNLTLMALGSSAPEILLS
	P.troglodytes	XP_001137342.1	WNETVSNLTLMALGSSAPEILLS
	M.mulatta	NP_001028033.1	WNETVSNLTLMALGSSAPEILLS
	C.lupus	XP_532945.3	WNETVSNLTLMALGSSAPEILLS
	B.taurus	NP_788805.1	WNETVSNLTLMALGSSAPEILLS
	M.musculus	NP_001106269.1	WNETVSNLTLMALGSSAPEILLS
	R.norvegicus	NP_062141.2	WNETVSNLTLMALGSSAPEILLS
	G.gallus	NP_001072941.1	WNETVSNLTLMALGSSAPEILLS
	D.rerio	NP_001034233.1	WNETVSNLTLMALGSSAPEILLS
	C.elegans	NP_001041182.1	WNETVSNLTLMALGSSAPEILLS
SLC8A2	H.sapiens	NP_055878.1	WNETVSNLTLMALGSSAPEILLS
	C.lupus	XP_541535.4	WNETVSNLTLMALGSSAPEILLS
	B.taurus	XP_002695230.2	WNETVSNLTLMALGSSAPEILLS
	M.musculus	NP_683748.1	WNETVSNLTLMALGSSAPEILLT
	R.norvegicus	NP_511174.1	WNETVSNLTLMALGSSAPEILLS
	D.rerio	NP_001116756.1	WNETVSNLTLMALGSSAPEILLS
SLC8A3	H.sapiens	NP_489479.1	WNETVSNLTLMALGSSAPEILLS
	P.troglodytes	XP_001144620.1	WNETVSNLTLMALGSSAPEILLS
	M.mulatta	XP_001110866.1	WNETVSNLTLMALGSSAPEILLS
	C.lupus	XP_853514.1	WNETVSNLTLMALGSSAPEILLS
	B.taurus	NP_001178128.1	WNETVSNLTLMALGSSAPEILLS
	M.musculus	NP_536688.2	WNETVSNLTLMALGSSAPEILLS
	R.norvegicus	NP_511175.1	WNETVSNLTLMALGSSAPEILLS
	G.gallus	XP_001231414.2	WNETVSNLTLMALGSSAPEILLS
	D.rerio	NP_001116728.1	WNETVSNLTLMALGSSAPEILLS
	C.elegans	NP_504415.2	WNDTVSNLTLMALGSSAPEILLS
	A.thaliana	NP_566105.1	WNFTIADISLLAFGTSFPQISLA
	O.sativa	NP_001068402.1	WNYTIADVALLAFGTSFPQISLA

Appendix Figure 6.
SLC24A4 gene structure and disease-causing mutations. The 3 *SLC24A4* gene structures correspond to the 3 *SLC24A4* transcript variants (TV) listed in GenBank TV1: NM_153646.3; TV2: NM_153647.3; TV3: NM_153648.3 and are based upon the *SLC24A4* genomic reference sequence NG_023408.1. The 17 numbered boxes are exons. Introns are indicated by a black line. The intron and exon lengths are not drawn to scale. The numbers below each exon indicate the range of amino acids encoded by each exon. Darkened areas are non-coding. The gene and cDNA and mutation descriptions are based upon *SLC24A4* reference sequences NG_023408.1 and NM_153646.3, respectively.

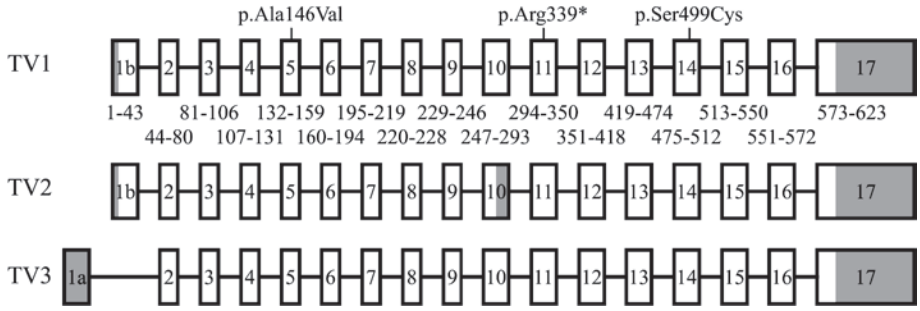

SLC24A4 mutations causing Autosomal Recessive AI (ARAI)

Location	Gene	cDNA	Protein	Reference
1. Exon 5	g.124552C>A	c.437C>T	p.Ala146Val	This Report
2. Exon 11	g.136454C>G	c.1015C>T	p.Arg339*	(Parry et al., 2013)
3. Exon 14	g.169158A>G	c.1495A>T	p.Ser499Cys	(Parry et al., 2013)

Appendix References

Bohm J, Chevessier F, Maues De Paula A, Koch C, Attarian S, Feger C, *et al.* (2013). Constitutive activation of the calcium sensor STIM1 causes tubular-aggregate myopathy. *Am J Hum Genet* 92:271-278.

Byun M, Abhyankar A, Lelarge V, Plancoulaine S, Palanduz A, Telhan L, et al. (2010). Whole-exome sequencing-based discovery of STIM1 deficiency in a child with fatal classic Kaposi sarcoma. *J Exp Med* 207:2307-2312.

Feske S, Picard C, Fischer A (2010). Immunodeficiency due to mutations in ORAI1 and STIM1. *Clin Immunol* 135:169-182.

Fuchs S, Rensing-Ehl A, Speckmann C, Bengsch B, Schmitt-Graeff A, Bondzio I, *et al.* (2012). Antiviral and regulatory T cell immunity in a patient with stromal interaction molecule 1 deficiency. *J Immunol* 188:1523-1533.

McCarl CA, Picard C, Khalil S, Kawasaki T, Rother J, Papolos A, *et al.* (2009). ORAI1 deficiency and lack of store-operated Ca2+ entry cause immunodeficiency, myopathy, and ectodermal dysplasia. *J Allergy Clin Immunol* 124:1311-1318. 7.

Muik M, Fahrner M, Schindl R, Stathopulos P, Frischauf I, Derler I, *et al.* (2011). STIM1 couples to ORAI1 via an intramolecular transition into an extended conformation. *EMBO J* 30:1678-1689.

Parry DA, Poulter JA, Logan CV, Brookes SJ, Jafri H, Ferguson CH, *et al.* (2013). Identification of mutations in SLC24A4, encoding a potassium-dependent sodium/calcium exchanger, as a cause of amelogenesis imperfecta. *Am J Hum Genet* 92:307-312.

Picard C, McCarl CA, Papolos A, Khalil S, Luthy K, Hivroz C, *et al.* (2009). STIM1 mutation associated with a syndrome of immunodeficiency and autoimmunity. *N Engl J Med* 360:1971-1980.

STIM1 and *SLC24A4* Are Critical for Enamel Maturation

S. Wang, M. Choi, A.S. Richardson, B.M. Reid, F. Seymen, M. Yildirim, E. Tuna, K. Gençay, J.P. Simmer and J.C. Hu

J DENT RES 2014 93: 94S originally published online 12 March 2014
DOI: 10.1177/0022034514527971

CLINICAL INVESTIGATIONS

STIM1 and *SLC24A4* Are Critical for Enamel Maturation

S. Wang[1,2], M. Choi[3,4]*, A.S. Richardson[1], B.M. Reid[1], F. Seymen[5], M. Yildirim[5], E. Tuna[5], K. Gençay[5], J.P. Simmer[1]*, and J.C. Hu[1]

Abstract: *Dental enamel formation depends upon the transcellular transport of Ca^{2+} by ameloblasts, but little is known about the molecular mechanism, or even if the same process is operative during the secretory and maturation stages of amelogenesis. Identifying mutations in genes involved in Ca^{2+} homeostasis that cause inherited enamel defects can provide insights into the molecular participants and potential mechanisms of Ca^{2+} handling by ameloblasts. Stromal Interaction Molecule 1 (STIM1) is an ER transmembrane protein that activates membrane-specific Ca^{2+} influx in response to the depletion of ER Ca^{2+} stores. Solute carrier family 24, member 4 (SLC24A4), is a $Na^+/K^+/Ca^{2+}$ transporter that exchanges intracellular Ca^{2+} and K^+ for extracellular Na^+. We identified a proband with syndromic hypomaturation enamel defects caused by a homozygous C to T transition (g.232598C>T c.1276C>T p.Arg426Cys) in* STIM1*, and a proband with isolated hypomaturation enamel defects caused by a homozygous C to T transition (g.124552C>T; c.437C>T; p.Ala146Val) in* SLC24A4*. Immunohistochemistry of developing mouse molars and incisors showed positive STIM1 and SLC24A4 signal specifically in maturation-stage ameloblasts. We conclude that enamel maturation is dependent upon STIM1 and SLC24A4 function, and that there are important differences in the Ca^{2+} transcellular transport systems used by secretory- and maturation-stage ameloblasts.*

Key Words: inherited diseases, mutations, tooth, calcium, amelogenesis imperfecta.

Introduction

The thickness of the enamel layer covering the crowns of teeth is determined by appositional growth during the secretory stage of amelogenesis, which is characterized by the deposition, on the enamel surface, of mineral ribbons that elongate outward, expanding the enamel layer until it reaches its final thickness (Simmer *et al.*, 2010). The hardness of dental enamel depends upon the thickening and interlocking of adjacent crystallites, which occurs during the maturation stage, and requires the removal of matrix protein remnants and the influx and efflux of ions. More than 60% of mineral deposition takes place during enamel maturation (Smith, 1998), and disturbances in matrix removal and ion transport cause hardness defects in dental enamel.

Transcellular transport of Ca^{2+} is a critical process during amelogenesis. Ca^{2+} enters tall, columnar, polarized ameloblasts proximally at the blood supply and exits distally into the developing enamel extracellular space to form calcium hydroxyapatite. Radiolabeled calcium (^{45}Ca) injected into the vascular system passes rapidly through both secretory- (Munhoz and Leblond, 1974) and maturation- (Reith *et al.*, 1984) stage ameloblasts and accumulates in developing enamel. The short transit times for the passage of ^{45}Ca through the enamel organ during both of these stages suggested that the same mechanism for calcium transcellular transport was shared by secretory- and maturation-stage ameloblasts (Reith *et al.*, 1984).

Stromal Interaction Molecule 1 (STIM1) is a transmembrane protein with Ca^{2+} binding domains in the endoplasmic reticulum (ER) that is activated by depletion of ER Ca^{2+} stores (Feske, 2009). After store-emptying, STIM1 forms multimers that passively migrate to ER-plasma membrane junctions, where they activate the Ca^{2+} channel ORAI1 (Singaravelu *et al.*, 2011). Together, STIM1 and ORAI1 mediate store-operated calcium entry (SOCE), which is a Ca^{2+} influx pathway critical for the normal functioning of many cell types, including

DOI: 10.1177/0022034514527971. [1]Department of Biologic and Materials Sciences, University of Michigan School of Dentistry, 1210 Eisenhower Place, Ann Arbor, MI, USA; [2]Oral Health Sciences Program, University of Michigan School of Dentistry, 1011 North University, Ann Arbor, MI, USA; [3]Department of Biomedical Sciences, College of Medicine, Seoul National University, 275-1 Yongon-dong, Chongno-gu, Seoul 110-768, Korea; [4]Department of Genetics, Howard Hughes Medical Institute, Yale University School of Medicine, 333 Cedar Street, New Haven, CT, USA; and [5]Department of Pedodontics, Istanbul University, Faculty of Dentistry, Istanbul, Turkey; *corresponding authors, jsimmer@umich.edu, murimchoi@snu.ac.kr

A supplemental appendix to this article is published electronically only at http://jdr.sagepub.com/supplemental.

T-cells, muscle cells, and ameloblasts. Homozygous loss of function mutations in *ORAI1* (Feske *et al.*, 2006; McCarl *et al.*, 2009) and *STIM1* (Picard *et al.*, 2009) cause Immunodeficiency 9 and 10 (IMD9, #612783; IMD10, MIM #612783), respectively, which feature severe immunodeficiency, congenital myopathy, ectodermal dysplasia, and enamel defects. *STIM1* is expressed by the soft tissue overlying developing enamel and showed an 8-fold increase in tissues overlying maturation-stage relative to those overlying secretory-stage enamel (Lacruz *et al.*, 2012).

Despite the association of human *STIM1* and *ORAI1* mutations with developmental enamel defects and the importance of transcellular Ca^{2+} transport for enamel formation, little is known about the role played by store-operated calcium entry (SOCE) in amelogenesis. *Stim1* knockout mice show 70% perinatal lethality. Surviving animals have a maximum life span of about 6 wks (Varga-Szabo *et al.*, 2008), but none of the *Stim1* knockout mouse reports commented on the dentition. There are only a few reported *STIM1* (Appendix Fig. 1) and *ORAI1* mutations, and only 2 oral photographs (one each) in the literature (McCarl *et al.*, 2009; Fuchs *et al.*, 2012) (Appendix Fig. 2).

An ion transporter involved in Ca^{2+} efflux is also associated with enamel defects. *SLC24A4* belongs to a family of potassium-dependent sodium-calcium exchanger, which has 5 members, *SLC24A1* through *SLC24A5* (Lytton, 2007). Olfactory-specific *Slc24a4* null mice have difficulty locating an odorous source (Stephan *et al.*, 2011), while *Slc24a4* null mice display enamel malformations, and defects in human *SLC24A4* cause a hypomaturation form of autosomal-recessive amelogenesis imperfecta (AI) (Parry *et al.*, 2013). *Slc24a4* is expressed by maturation-stage ameloblasts, and the protein tends to localize along the ameloblast distal membrane adjacent to the mineral layer (Hu *et al.*, 2012).

In this study we identify novel homozygous *STIM1* and *SLC24A4* mutations that cause autosomal-recessive hypomaturation enamel malformations and characterize the expression of STIM1 and SLC24A4 in developing mouse teeth. The results provide insight into a possible mechanism for calcium transport through ameloblasts during enamel maturation.

Methods

The human study protocol and consents were reviewed and approved by the Ethics Committee at the University of Istanbul, Turkey, and by the Institutional Review Board at the University of Michigan. Study participants signed appropriate written consents after explanation and discussion of their contents. All animal procedures were approved by the University of Michigan Committee of Use and Care of Animals.

Mutational Analysis

Genomic DNA from the *STIM1* proband was submitted to the Yale Center for Genome Analysis (YCGA, West Haven, CT, USA), and genomic DNA from the *SLC24A4* proband was submitted to Edge BioSystems (Gaithersburg, MD, USA) for whole-exome sequencing. Reads were aligned to the human reference genome hg19 by ELAND v2. Single-nucleotide variants and short insertions and deletions (indels) were called using SAMtools. The called variants were annotated with an in-house script. The annotated results were inspected for potential disease-causing sequence variations in the following candidate genes: *AMELX, ENAM, FAM83H, KLK4, MMP20, WDR72, FAM20A, C4orf26, SLC24A4, CNNM4, AMBN, ITGB6, AMTN, ODAM, SP6, COL17A1, ROGDI, LAMA3, LAMB3, LAMC2, DLX3, GJA1, AIRE*, and *ABCC6*.

Since the *STIM1* kindred reported consanguinity, recessive mutations were assumed, and 8 novel rare protein-altering homozygous variants were identified (Appendix Fig. 3). These were assessed for PhyloD score and by PolyPhen prediction. Their frequencies in the YCGA and 1000 Genomes databases and possible genetic associations in the OMIM database were taken into account. *STIM1* exon 10 and *SLC24A4* exon 5, inclusive of adjoining intron sequences, were amplified from all recruited members of the respective kindreds and characterized by Sanger DNA sequencing.

Immunohistochemistry

Immunohistochemistry on days 5, 11, and 14 mouse heads was carried out as described previously (Wang *et al.*, 2014), with an anti-STIM1 antibody (1:100, HPA012123, Sigma-Aldrich, St. Louis, MO, USA) or an anti-SLC24A4 antibody (1:100, ab136968, Abcam, Cambridge, MA, USA). In brief, we used an anti-rabbit IgG secondary antibody conjugated with Alexa Fluor 594 (Invitrogen, Carlsbad, CA, USA). Cell nuclei were stained with DAPI (Invitrogen). The sections were examined under an Olympus BX51 with fluorescence attachments and photographed with an Olympus DP71 camera with DP controller and manager software.

Results

STIM1 Family

The proband was a 6-year-old female of Turkish decent who presented at the Department of Pedodontics at Istanbul University with a chief complaint related to her dental condition. The proband was the only affected person in the family, suggesting that the disorder was either sporadic or recessive. A pedigree was constructed based upon an interview with the parents and revealed consanguinity (Fig. 1A). The sizes and shapes of the dental crowns were within normal limits, but the enamel was creamy-brown and showed rapid attrition that had resulted in the loss of the maxillary central incisors (Fig. 1B). Both the primary and secondary dentitions were affected. Nail dysplasia was evident on the feet and hands (Fig. 1C). The proband had a history of frequent throat infections, but no immunological evaluation was performed. The family moved to another country, and contact was lost. Whole-exome analysis of the proband's genomic DNA identified a C to T transition (g.232598C>T c.1276C>T p.Arg426Cys) in both *STIM1* alleles. Sanger sequencing demonstrated that both parents were heterozygous for this

Figure 1.
STIM1 family. **(A)** Pedigree. Dots mark the three persons who donated samples for DNA sequencing. (**B)** Oral photographs of the proband (IV:1) at age 6 yrs. The teeth are normal in size and shape, but are brown or cream-colored, and have undergone attrition. (**C)** Photographs of the hands and feet showing nail dysplasia. (**D)** Sequence from *STIM1* Exon 10 revealing heterozygosity for the sequence variation g.232598C>T; c.1276C>T; p.Arg426Cys that occurred in the father (III:6) and mother (III:7) (top) and homozygosity in the proband (IV:1) (bottom). The mutation designations are with respect to the *STIM1* genomic reference sequence NG_016277.1 and cDNA reference sequence NM_001277961.1 (for mRNA transcript variant 1). Key: arrowhead, mutation point; Y, T or C.

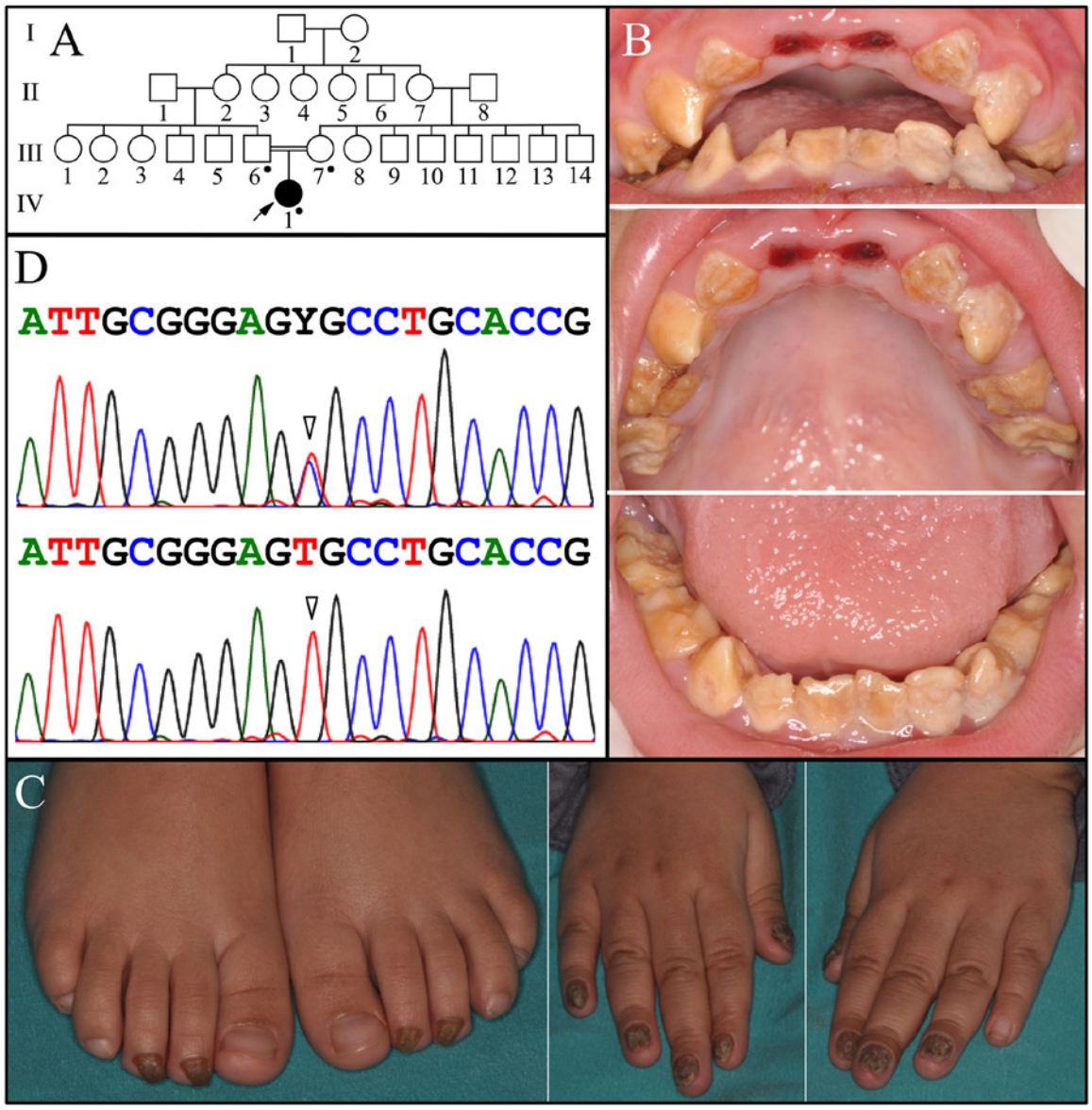

variation and confirmed that the proband was homozygous (Fig. 1D). The pattern of inheritance was therefore recessive.

Substantial evidence supports the conclusion that the STIM1 p.Arg426Cys substitution was disease-causing. The mutated position (Arg^{426}) is strictly conserved among STIM1 homologues going back to fish (Appendix Fig. 4A) and is located within the STIM1 ORAI1-activating region that extends from amino acids 347 to 438 (conserved domain cd11722). Besides Arg^{426} being conserved, the substitution of Arg^{426} with leucine in recombinant STIM1 prevented it from interacting with ORAI1 (Muik *et al.*, 2011). Transfection with a plasmid construct in HEK293 cells that expressed STIM1 amino acids 233 through 474 constitutively activated ORAI1, whereas the STIM1 construct expressing a p.Arg426Leu substitution failed to interact with ORAI1 (Muik *et al.*, 2011). PolyPhen-2 (Polymorphism Phenotyping v2) analysis of the p.Arg426Cys substitution gave a score of 1.0. Given that the proband suffers from a disease

Figure 2.
STIM1 immunohistochemistry of day 11 maxillary molars and a day 14 mandibular incisor. **(A)** Low-magnification (40×) views of the maxillary first (M1), second (M2), and third (M3) molars. Boxes outline the higher-magnification (100×) views in panels B and C. **(B)** Maxillary first molar (M1) at 100×. The box outlines the higher-magnification (200×) view in panel D. **(C)** Maxillary second (M2) and third (M3) molars at 100×. The box outlines the highest-magnification (400×) view shown in panel F. **(D)** Distal cusp of M1 (200×). The box outlines the highest-magnification (400×) view shown in panel E. **(E)** Distal cusp tip of M1 (400×). **(F)** Mesial cusp tip of M2 (400×). **(G)** Longitudinal sections of a mandibular incisor (400×). Arrowhead marks the approximate onset of the maturation stage. Note that only maturation-stage ameloblasts are positive for STIM1 in developing teeth. Secretory-stage ameloblasts in M3 and the incisor are negative. Key: Am, ameloblasts; P, pulp; SI, stratum intermedium.

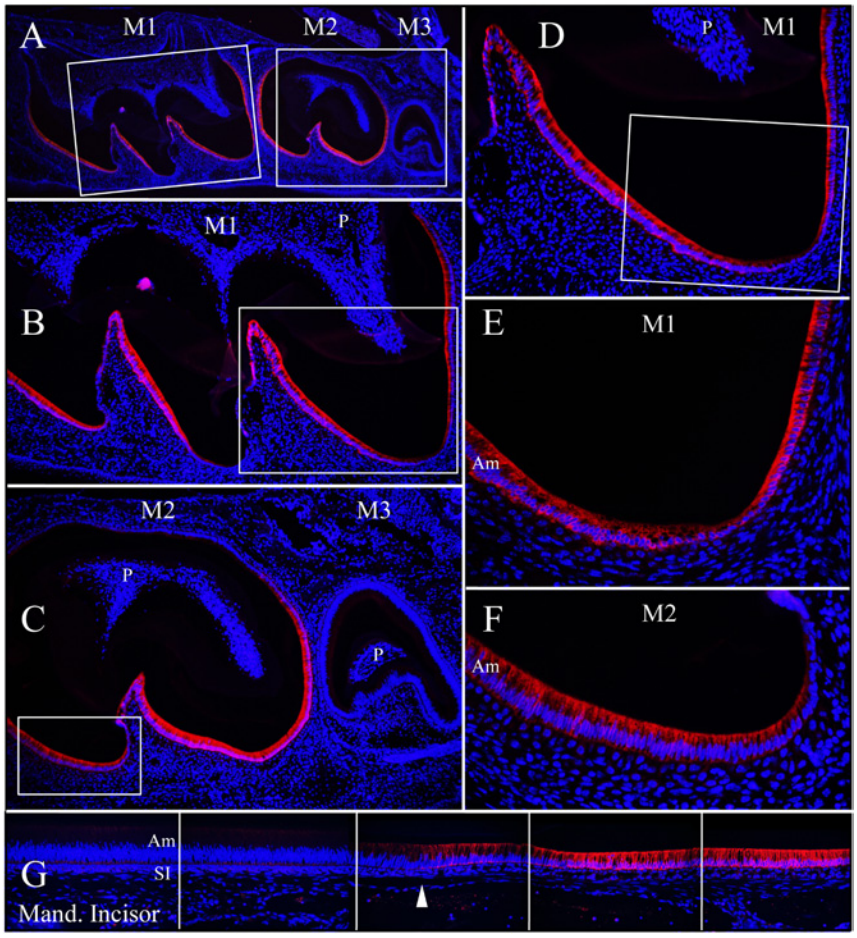

known to be caused by defects in *STIM1*, we conclude that the p.Arg426Cys substitution in STIM1 is disease-causing.

STIM1 immunohistochemistry of developing teeth in the day 11 mice localized STIM1 only in maturation-stage ameloblasts (Fig. 2). By day 11, ameloblasts in the maxillary first and second molars are in the maturation stage, while ameloblasts in the third molar and in the basal third of the incisor are in the secretory stage. Only maturation-stage ameloblasts were above the threshold for detection (positive) for STIM1. Odontoblasts, dental pulp cells, and all cells of the enamel organ epithelia (EOE) except maturation-stage ameloblasts were below threshold for detection (negative) for STIM1.

There are 3 transcript variants for human *STIM1* in GenBank (NM_001277961.1; NM_003156.3; NM_001277962.1) that express *STIM1* mRNA encoding 791, 685, and 540 amino acids, respectively. These transcripts are identical for the first 10 exons but differ in the length of exon 11 due to alternative splicing. We amplified mouse *Stim1* mRNA from exon 10 to exon 12 by reverse transcription-polymerase chain-reaction (RT-PCR) using RNA isolated from the EOE dissected from day 5 (secretory stage) and day 11 (maturation stage) mandibular first molars. *Stim1* amplified from both samples and the predominant *Stim1* expression product was analogous to human transcript variant 2 (Appendix Fig. 4B; day 5 not shown).

SLC24A4 Family

The proband, a 5.5-year-old Turkish girl, was the offspring of a first-cousin marriage and presented with enamel malformations. She was otherwise healthy and was the only individual with enamel defects in the family, suggesting that the disorder was caused by a recessive or sporadic mutation (Fig. 3A). She had a complete primary dentition with congenital fusion of the lower right deciduous lateral incisor and canine (teeth Q and R). The enamel was soft, creamy-yellow, and tended to chip. Extensive caries was observed (Fig. 3B). Radiographically, all of the tooth germs for the permanent dentition were present except the third molars and a missing tooth #26. The enamel of erupting incisors and first molars showed full thickness but did not contrast with the underlying dentin on radiographs (Fig. 3C). Whole-exome sequencing of the proband's genome identified a homozygous C to T transition (g.124552C>A; c.437C>T; p.Ala146Val) in *SLC24A4* and no other potential disease-causing mutations among the known AI candidate genes. Both parents were heterozygous for this variation, which demonstrated a recessive pattern of inheritance (Fig.

Figure 3.
SLC24A4 family. **(A)** Pedigree. The arrowhead marks the proband, the only affected individual in the consanguineous family. Dots mark the three persons who donated samples for DNA sequencing. **(B)** Oral photographs of the proband (II:1) at age 5.5 yrs. The teeth are yellow or cream-colored, and show signs of attrition and dental caries. **(C)** Panorex of the proband at age 5.5 yrs. The enamel of erupting first molars exhibits normal thickness but no contrast with underlying dentin, indicating maturation enamel defects. **(D)** Sequence from *SLC24A4* exon 5 showing the heterozygosity of the sequence variation g.124552C>A; c.437C>T; p.Ala146Val that occurred in the father (I:1) and mother (I:2) (left) and the homozygosity in the proband (II:1) (right). The mutation designations are with respect to the *SLC24A4* genomic reference sequence NG_023408.1 and cDNA reference sequence NM_153646.3 (for mRNA transcript variant 1). Key: arrowhead, mutation point; Y, T or C.

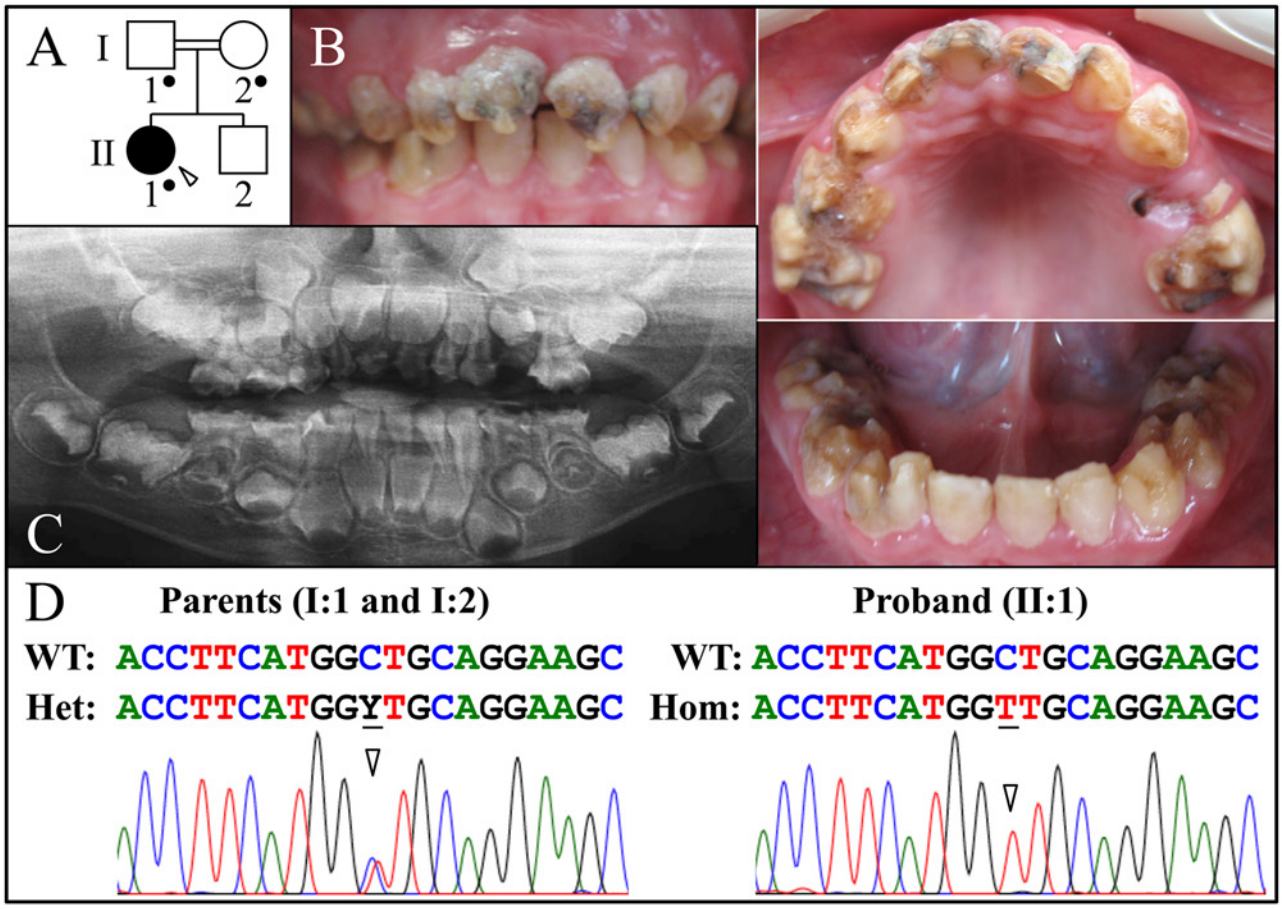

3D). The missense mutation substituted an extremely conserved SLC24A4 amino acid residue (Ala^{146}) that was predicted to be "probably damaging" (0.987 in HumDiv, 0.977in HumVar) by PolyPhen-2 analysis and could not be found in the dbSNP (build 137), 1000 Genome Project, or NHLBI Exome Sequencing Project databases.

SLC24A4 belongs to a superfamily of Na^+/Ca^{2+} exchangers that, in humans, includes the SLC8 and SLC24 families, and SLC24A6 (now SLC8B1), which is evolutionarily more distant (Lytton, 2007). This superfamily shares especially high sequence similarity within 2 internal hydrophobic domains (the α1- and α2-repeats). The *SLC24A4* mutation (p.Ala146Val) we identified replaces Ala^{146} in the α1-repeat, a position that is strictly conserved among SLC24A and SLC8A homologs (Appendix Fig. 5). Scanning mutagenesis of the corresponding alanine within the α1-repeat of SLC24A2 (p.Ala181Ser and p.Ala181Cys) reduced ion-exchange activity to 40% and 10% of that shown by the wild-type sequence, respectively (Winkfein *et al.*, 2003). Therefore, we conclude that the p.Ala146Val substitution in *SLC24A4* is disease-causing, the third to be reported (Appendix Fig. 6).

SLC24A4 immunohisto-chemistry showed strong signal in maturation ameloblasts (Fig. 4A) but was below detection in other tissues, including secretory ameloblasts, odontoblasts, pulp tissue, and bone (Figs. 4A-4C). In maturation-stage ameloblasts, SLC24A4 localized at the distal membrane and in the cytoplasm (Figs. 4D, 4E). Day 11 developing mouse teeth showed the

Figure 4.
SLC24A4 immunohistochemistry of developing teeth of mice at days 5 and 11. **(**A-E) At post-natal day 5 (PN5), SLC24A4 signal was observed in maturation-stage ameloblasts at the incisal end of the mandibular incisor and cusp tip of the first molar, and in skeletal muscles **(A).** High-magnification views of differentiation and secretory-stages toward the basal end of the mandibular incisor **(B, C);** transition to maturation stage **(D);** maturation stage **(E). (F-H)** At post-natal day 11 (PN11), SLC24A4 signal was detected in the maxillary first molar, where ameloblasts are in the maturation stage. (**I-K)** At post-natal day 11 (PN11), only ameloblasts of the mandibular first and second molars (at maturation stage) were above the threshold for detection, but other tissues, including secretory-stage ameloblasts (in the third molar and in the basal third of the incisor), were not (I). High magnification of secretory-stage ameloblasts in a mandibular incisor (J, K). Key: Am, ameloblasts; Inc, incisor; M1, first molar; M2, second molar; Od, odontoblasts; P, pulp; SI, stratum intermedium.

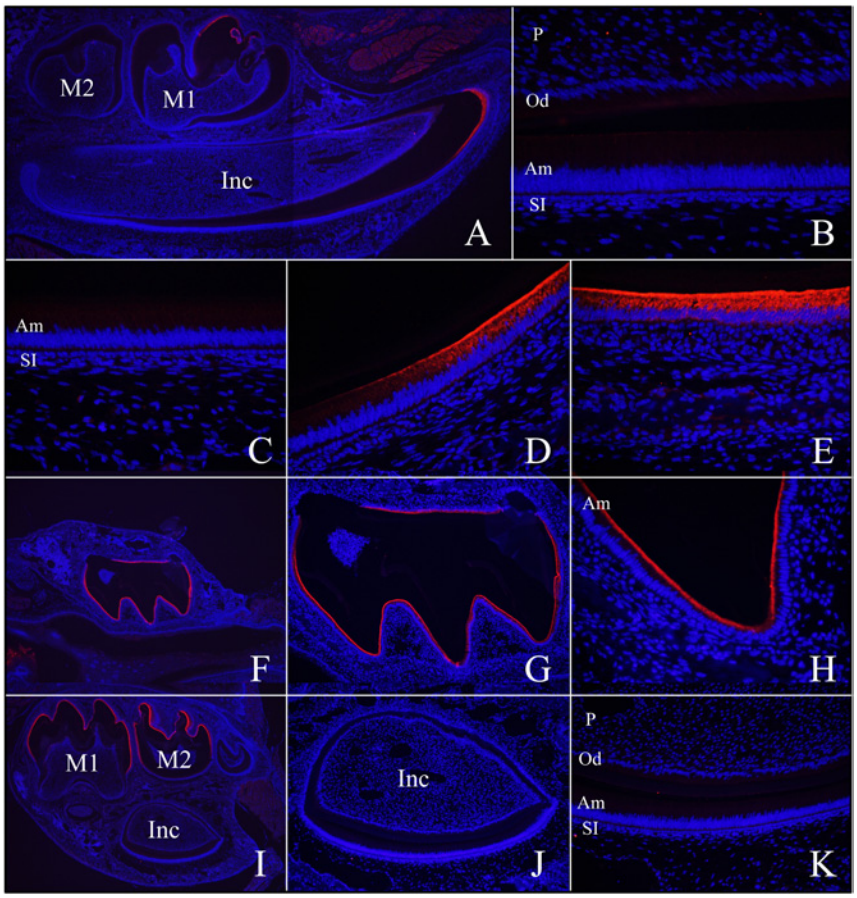

same stage-specific pattern of expression as the day 5 mice. Only maturation-stage ameloblasts (in the first and second molars) and skeletal muscles were above the threshold for detection (positive), but other tissues, including secretory-stage ameloblasts (in the third molar and in the basal third of the incisor), were not.

Discussion

The N-terminal portion of STIM1 contains paired EF hands that bind Ca^{2+} and allow STIM1 to sense and respond to the depletion of ER calcium stores. Recently, 4 heterozygous *STIM1* missense mutations in exons 2 and 3 encoding the EF hands were reported to trigger constitutive activation of STIM1, causing autosomal-dominant tubular-aggregate myopathy (TAM; MIM #160565) (Bohm *et al.*, 2013) with no mention of enamel malformations. Myoblasts showed elevated basal Ca^{2+} levels and dysregulation of intracellular Ca^{2+} homeostasis, indicating that tight regulation of STIM1-dependent store-operated Ca^{2+} entry is required for normal skeletal-muscle structure and function. In the recessive loss-of-function condition (IMD10), the phenotype results from failure of STIM1 to induce Ca^{2+} influx in response to ER calcium store depletion, resulting in lower than normal intracellular calcium levels. This impairs enamel maturation. In the dominant constitutive activation of STIM1 condition, a constant signal of depleted ER Ca^{2+} stores results in elevated intracellular Ca^{2+} levels, which does not appear to affect enamel maturation (Bohm *et al.*, 2013). Perhaps maturation-stage ameloblasts are less sensitive to elevated basal Ca^{2+} levels than are muscle cells, or the excess can be shunted into the forming enamel.

Many proteins associated with Ca^{2+} transport are expressed in ameloblasts, including members of the plasma membrane Ca^{2+} ATPase (PMCA, *ATP2B*), Na^{+}/Ca^{2+} exchanger (NCX, *SLC8A*), and Na^{+}/Ca^{2+}-K^{+} exchanger (NCKX, *SLC24A*) families (Borke *et al.*, 1995; Okumura *et al.*, 2010). Some of these proteins are expressed in many tissues and play critical roles in cell physiology, such as ATP2B1 and SLC8A1, but most show differential or tissue-specific distributions, and aberration of these proteins leads to human diseases in specific organs. For example, mutations in *ATP2B2* cause autosomal-recessive deafness (Schultz *et al.*, 2005), and *SLC24A1* mutations cause congenital stationary night blindness (Riazuddin *et al.*, 2010). Despite the expression of several calcium transport proteins in ameloblasts, little evidence has supported that they are necessary for amelogenesis until it was recently reported that mutations in *SLC24A4* cause enamel malformations

(Parry *et al*., 2013). In this study, we identify the third *SLC24A4* mutation in a patient with isolated hypomaturation AI. SLC24A4 immunohistochemistry of Day 5 and Day 11 developing mouse teeth localized SLC24A4 almost exclusively in maturation-stage ameloblasts, which strongly suggests that SLC24A4 has a critical function during enamel maturation. Since STIM1 and SLC24A4 are both specific to and critical for the maturation stage, there must be important differences in the Ca^{2+} transport systems used by secretory- and maturation-stage ameloblasts.

The genetic findings suggest a working hypothesis that explains how Ca^{2+} from the blood supply might be drawn through maturation-stage ameloblasts to support mineralization. The Ca^{2+} and PO_4^{3-} concentrations in the "enamel fluid" in the enamel extracellular compartment are nearly as low as they can be and still support mineralization (Aoba and Moreno, 1987). Perhaps low extracellular Ca^{2+} activity in the matrix facilitates the active transport of calcium ions out of the cell and into the enamel matrix through SLC24A4 (using the energy of a Na^+ gradient). This efflux might lower intracellular Ca^{2+}, deplete ER stores, and activate the SOCE system (STIM1/ORAI1) to replenish intracellular Ca^{2+} stores by channeling Ca^{2+} entry on the proximal side of maturation-stage ameloblasts, nearest the blood supply.

Acknowledgments

We thank the participants in this study. This work was supported by the National Institute of Dental and Craniofacial Research of the National Institutes of Health (NIDCR/NIH Grant DE015846). The authors declare no potential conflicts of interest with respect to the authorship and/or publication of this article.

References

Aoba T, Moreno EC (1987). The enamel fluid in the early secretory stage of porcine amelogenesis: chemical composition and saturation with respect to enamel mineral. *Calcif Tissue Int* 41:86-94.

Bohm J, Chevessier F, Maues De Paula A, Koch C, Attarian S, Feger C, *et al.* (2013). Constitutive activation of the calcium sensor STIM1 causes tubular-aggregate myopathy. *Am J Hum Genet* 92:271-278.

Borke JL, Zaki A el-M, Eisenmann DR, Mednieks MI (1995). Localization of plasma membrane Ca2+ pump mRNA and protein in human ameloblasts by in situ hybridization and immunohistochemistry. *Connect Tissue Res* 33:139-144.

Feske S (2009). ORAI1 and STIM1 deficiency in human and mice: roles of store-operated Ca2+ entry in the immune system and beyond. *Immunol Rev* 231:189-209.

Feske S, Gwack Y, Prakriya M, Srikanth S, Puppel SH, Tanasa B, *et al.* (2006). A mutation in Orai1 causes immune deficiency by abrogating CRAC channel function. *Nature* 441:179-185.

Fuchs S, Rensing-Ehl A, Speckmann C, Bengsch B, Schmitt-Graeff A, Bondzio I, *et al.* (2012). Antiviral and regulatory T cell immunity in a patient with stromal interaction molecule 1 deficiency. *J Immunol* 188:1523-1533.

Hu P, Lacruz RS, Smith CE, Smith SM, Kurtz I, Paine ML (2012). Expression of the sodium/calcium/potassium exchanger, NCKX4, in ameloblasts. *Cells Tissues Organs* 196:501-509.

Lacruz RS, Smith CE, Bringas P Jr, Chen YB, Smith SM, Snead ML, *et al.* (2012). Identification of novel candidate genes involved in mineralization of dental enamel by genome-wide transcript profiling. *J Cell Physiol* 227:2264-2275.

Lytton J (2007). Na+/Ca2+ exchangers: three mammalian gene families control Ca2+ transport. *Biochem J* 406:365-382.

McCarl CA, Picard C, Khalil S, Kawasaki T, Rother J, Papolos A, *et al.* (2009). ORAI1 deficiency and lack of store-operated Ca2+ entry cause immunodeficiency, myopathy, and ectodermal dysplasia. *J Allergy Clin Immunol* 124:1311-1318.e7.

Muik M, Fahrner M, Schindl R, Stathopulos P, Frischauf I, Derler I, *et al.* (2011). STIM1 couples to ORAI1 via an intramolecular transition into an extended conformation. *EMBO J* 30:1678-1689.

Munhoz CO, Leblond CP (1974). Deposition of calcium phosphate into dentin and enamel as shown by radioautography of sections of incisor teeth following injection of 45Ca into rats. *Calcif Tissue Res* 15:221-235.

Okumura R, Shibukawa Y, Muramatsu T, Hashimoto S, Nakagawa K, Tazaki M, *et al.* (2010). Sodium-calcium exchangers in rat ameloblasts. *J Pharmacol Sci* 112:223-230.

Parry DA, Poulter JA, Logan CV, Brookes SJ, Jafri H, Ferguson CH, *et al.* (2013). Identification of mutations in SLC24A4, encoding a potassium-dependent sodium/calcium exchanger, as a cause of amelogenesis imperfecta. *Am J Hum Genet* 92:307-312.

Picard C, McCarl CA, Papolos A, Khalil S, Luthy K, Hivroz C, *et al.* (2009). STIM1 mutation associated with a syndrome of immunodeficiency and autoimmunity. *N Engl J Med* 360:1971-1980.

Reith EJ, Schmid MI, Boyde A (1984). Rapid uptake of calcium in maturing enamel of the rat incisor. *Histochemistry* 80:409-410.

Riazuddin SA, Shahzadi A, Zeitz C, Ahmed ZM, Ayyagari R, Chavali VR, *et al.* (2010). A mutation in SLC24A1 implicated in autosomal-recessive congenital stationary night blindness. *Am J Hum Genet* 87:523-531.

Schultz JM, Yang Y, Caride AJ, Filoteo AG, Penheiter AR, Lagziel A, *et al.* (2005). Modification of human hearing loss by plasma-membrane calcium pump PMCA2. *N Engl J Med* 352:1557-1564.

Simmer JP, Papagerakis P, Smith CE, Fisher DC, Rountrey AN, Zheng L, *et al.* (2010). Regulation of dental enamel shape and hardness. *J Dent Res* 89:1024-1038.

Singaravelu K, Nelson C, Bakowski D, de Brito OM, Ng SW, Di Capite J, *et al.* (2011). Mitofusin 2 regulates STIM1 migration from the Ca2+ store to the plasma membrane in cells with depolarized mitochondria. *J Biol Chem* 286:12189-12201.

Smith CE (1998). Cellular and chemical events during enamel maturation. *Crit Rev Oral Biol Med* 9:128-161.

Stephan AB, Tobochnik S, Dibattista M, Wall CM, Reisert J, Zhao H (2011). The Na(+)/Ca(2+) exchanger NCKX4 governs termination and adaptation of the mammalian olfactory response. *Nat Neurosci* 15:131-137.

Varga-Szabo D, Braun A, Kleinschnitz C, Bender M, Pleines I, Pham M, *et al.* (2008). The calcium sensor STIM1 is an essential mediator of arterial thrombosis and ischemic brain infarction. *J Exp Med* 205:1583-1591.

Wang SK, Choi M, Richardson AS, Reid BM, Lin BP, Wang SJ, *et al.* (2014). ITGB6 loss of function mutations cause autosomal recessive amelogenesis imperfecta. *Hum Mol Genet* 23:2157-2163.

Winkfein RJ, Szerencsei RT, Kinjo TG, Kang K, Perizzolo M, Eisner L, *et al.* (2003). Scanning mutagenesis of the alpha repeats and of the transmembrane acidic residues of the human retinal cone Na/Ca-K exchanger. *Biochemistry* 42:543-552.